

Article

Design and Analysis of 15 MW SPM Vernier Generator for Direct-Drive Wind Turbine Applications

Abdur Rehman  and Byungtaek Kim * 

Department of Electrical Engineering, Kunsan National University, Gunsan 54150, Republic of Korea

* Correspondence: btkim@kunsan.ac.kr

Abstract: This paper presents the design and an analysis of a surface PM vernier generator (SPMVG) for MW-scale direct-drive (DD) wind turbine application. An SPMVG has the advantage of higher torque density; however, especially at higher power ratings with increased electrical loadings, the power factor worsens and there are some serious concerns including magnetic saturation of cores and PM demagnetization. These issues are directly related to machine design parameters such as PM dimensions, applied electrical loading, slot geometry and the choice of slot–pole combination. It is determined that depending on the PM thickness and a few other design variables, each slot–pole combination has an optimal value of specific electrical loading. The use of the optimal value of specific electrical loading ensures that the machine is not saturated, the performance is optimum and the power factor is not unnecessarily degraded. Moreover, under certain design constraints, design criteria are developed that ensure the proper choice of various entailed design variables. By using the developed design criteria, the trends of various electromagnetic performances with variation in the slot–pole combination are discussed. The obtained trends clearly show that each slot–pole combination offers a certain torque density and power factor; thus, it serves as a guide for the selection of the slot–pole combination considering the required torque density and/or certain power factor limit. Finally, by using the developed design approach, an SPMVG for rated power of 15 MW is designed; the design objectives are to maximize torque per volume with a power factor limit of 0.4. Moreover, the various aspects of the performances of the designed SPMVG are comprehensively compared against a conventional PM DD 15 MW generator.

Keywords: design; direct drive; MW scale; magnetic saturation; power factor; PM vernier; specific electric loading; torque per volume; wind generator



Citation: Rehman, A.; Kim, B. Design and Analysis of 15 MW SPM Vernier Generator for Direct-Drive Wind Turbine Applications. *Energies* **2023**, *16*, 1094. <https://doi.org/10.3390/en16031094>

Academic Editor: Davide Astolfi

Received: 20 December 2022

Revised: 10 January 2023

Accepted: 10 January 2023

Published: 19 January 2023



Copyright: © 2023 by the authors. Licensee MDPI, Basel, Switzerland. This article is an open access article distributed under the terms and conditions of the Creative Commons Attribution (CC BY) license (<https://creativecommons.org/licenses/by/4.0/>).

1. Introduction

Over the last decade, research and development related to the wind energy has grown very rapidly; in particular, research trends have been focused on multi-MW direct-drive (DD) offshore wind turbines [1–3]. The main motivation behind the upscaling of wind turbines is to lower the levelized cost of energy (LCOE). According to the Global Wind Energy Council 2022 report, 21.1 GW was added in the offshore market in 2021, three times more than in 2020, showing year-over-year growth of 58% [1]. Considering the reliability and energy yield, DD topology is preferred over the traditional geared wind turbine system [4]. However, direct-drive generators, due to the high torque requirements, suffer from large volume and higher material consumption which results in higher cost. To overcome these issues, it is necessary to use higher torque/power density generators.

Flux modulation machines (FMMs) owing to the flux modulation effects have higher torque densities and thus FMMs are naturally suitable for direct-drive applications [5–15]. Among the family of FMMs, the surface PM (SPM) vernier machine is famous due to its higher torque density, higher torque quality and simple mechanical structure [5,6]. Aside from the advantages, the low power factor of the SPM vernier machine, getting significantly

lower especially at higher power ratings (MW scale), remains a challenge and there are some serious concerns including magnetic saturation and PM demagnetization [11,13].

The SPM vernier machine is magnetically identical to a conventional PM machine with an integrated magnetic gear where the degree of the magnetic gearing effect is defined by the term gear ratio that is a function of the machine's slot-pole combination [7]. Due to the unique operation principle of the SPM vernier machine, it has certain design constraints that are not that relevant for regular PM machines [5]. From that point of view, the conventional design procedure based on the pre-set magnetic and electric loadings is not proper for flux modulation machines [7].

In the literature, the SPM vernier machine, due to its high torque density, has been discussed with regard to the application of direct-drive wind generators with power ratings up to a few kilowatts [7,9,12]. On the other hand, in recent years, the SPM vernier machine with an MW-scale power range has been considered in several studies [11,13–15]. In [11], the impact of scaling (from 3 kW to 3 MW) on the electromagnetic performance of the SPM vernier machine was investigated; it was indicated that the magnetic saturation especially at low slot-pole combinations is serious and of course there is a problem with regard to a poor power factor; these issues fundamentally arise due to the use of higher electrical loading [11]; similar issues concerning the SPM vernier machine are reported in [13,14]. Two SPM vernier models—with 1 and 3 MW—are optimally designed in [15] and the authors concluded that, considering the power factor and the total machine mass, an SPM vernier machine with lower gear ratios is more promising.

In previous studies related to the SPMVG for MW-scale wind turbine application, the design of the generator is largely based on numerical optimization, which greatly limits the extent of the insights into the nature of the design problem. Moreover, considering the numerous slot-pole combinations and the various entailed design parameters, it is not proper to utilize the numerical optimization methods at the pre-design stages. The fundamental issues of SPMVG that become more serious at higher power levels are related to the design parameters and the most important parameter is the specific electrical loading. It will be shown in this study that each slot-pole combination depending on certain design parameters has its own specific electrical loading value; unfortunately, the present literature has neglected addressing the matter from that point of view. In addition, with regard to the proper selection of various important design parameters, the general trends of the resulting electromagnetic performances have not yet been discussed and the scope of most studies is limited to a specific gear ratio. Therefore, in order to analyze the feasibility of SPMVG with regard to the MW scale, first it is important to establish a proper and systematic design procedure that clearly defines the ways to properly choose the various entailed design parameters.

With the aim of evaluating the feasibility of surface PM vernier generators (SPMVGs) for MW-scale wind turbine applications, this paper presents the design and an analysis of an outer rotor SPMVG. The fact that the SPMVG has higher torque density makes it suitable for DD applications; however, concerns such as its worse power factor and the magnetic saturation of cores that are more prominent at higher power ratings (MW scale) should be carefully considered. The severity of these issues depends on certain design parameters, including slot-pole combination, PM dimensions and the applied specific electric loading. In order to address these issues, the basic operation principle and the involved design variables are introduced, and the relations between important design aspects such as the selection of slot-pole combination, the PM dimensions and the choice of specific electrical loading are discussed. Based on certain design constraints, proper design criteria are developed ensuring the proper selection of various entailed design parameters. The various trends of key electromagnetic performance with variation of slot-pole combination are investigated. Finally, based on the proposed design criteria, an SPMVG for a rated power of 15 MW is designed under the design objectives of maximum torque density while having a power factor limit of 0.4. To clearly highlight the pros and cons of SPMVG, the

various aspects of the electromagnetic performances are comprehensively investigated and compared against a 15 MW DD SPM generator developed by NREL [3].

2. Basic Operation Principle and Analytical Modeling

Like all flux modulation machines, a SPM vernier machine also works on the principle of magnetic gearing effect, alternatively called the flux modulation effect [5]. In order to utilize the flux modulation effect, the stator windings should be configured to obtain a 3-phase balanced back EMF E_{ph} from the modulation flux whose number of pole pairs p_{mod}^- is given as $Z_s - Z_r$, where Z_r and Z_s represent the number of PM pole pairs and stator slots, respectively. The ratio of Z_r to p_{mod}^- is defined as gear ratio G_r , and the choice of both p_{mod}^- and G_r are crucial in order to effectively utilize the flux modulation effects.

The basic structure of SPMVG in outer rotor configuration along with the important design variables is shown in Figure 1. The stator of the structure shown in Figure 1 is installed with the most common fractional slot winding configuration having the ratio of 3 slots/2 poles, where the number of poles means the modulation poles, not the actual PM poles. Moreover, the stator of the machine has Q_s main slots for the windings and each slot has auxiliary teeth n_{aux} , and therefore the total number of slots is $Z_s = n_{aux}Q_s$.

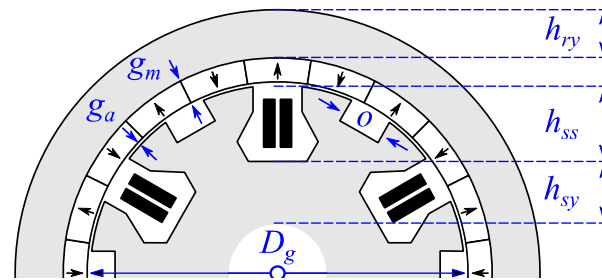


Figure 1. Basic structure of SPMVG.

2.1. Air-Gap Flux Density and Back EMF

For the structure shown in Figure 1, the air-gap magneto-motive force (MMF) developed by the PMs and the specific air-gap permeance can be expressed as (1) and (2), respectively, where F_{m1} is the magnitude of the 1st component of the air-gap MMF [5] due to the PMs. In (2), the average permeance P_0 and the first harmonic permeance P_1 are expressed in terms of the air-gap geometries as (3) and (4), respectively, where g_{eff} is the effective air-gap length, c_0 is the ratio of slot opening o to slot pitch t_d , and β is given in (5).

$$F_{gm}(\theta, \theta_m) \approx F_{m1} \cos(Z_r(\theta - \theta_m)) \tag{1}$$

$$P_g(\theta, \theta_m) \approx P_0 - P_1 \cos(Z_s\theta) \tag{2}$$

$$P_0 = \frac{\mu_0}{g_{eff}} (1 - 1.6\beta c_0) \tag{3}$$

$$P_1 = \frac{\mu_0}{g_{eff}} \frac{2\beta}{\pi} \left(\frac{0.39}{0.39 - c_0^2} \right) \sin(1.6\pi c_0) \tag{4}$$

$$\beta = \frac{1}{2} - \left\{ \sqrt{4 + \left(\frac{o}{g_{eff}} \right)^2} \right\}^{-1} \tag{5}$$

By using the air-gap MMF of (1) and air-gap permeance of (2), the air-gap flux density due to the PM can be expressed as (6), where the main flux $B_0 = F_{m1}P_0$ and the modulation flux $B_1 = 0.5F_{m1}P_1$, $p_{mod}^\pm = |Z_s \pm Z_r|$. The third term in (3) with p_{mod}^+ has negligible contribution due to its very low speed; however, here, in this study, for the sake of accurate modeling, p_{mod}^+ is not neglected. As the magnitude of the modulation flux B_1 is related

with the F_{m1} and the harmonic permeance P_1 and both P_1 and F_{m1} are linked with the PM thickness and specifically as given by (4), P_1 also depends on the choice of stator slot opening ratio c_0 and the value of β . Therefore, to effectively utilize the modulation flux, the choice of PM thickness g_m and c_0 is important. Considering the magnitude of P_1 the optimal value of stator slot opening ratio c_0 lies somewhere around 0.5~0.6 [5], in this study, the value of c_0 is set as 0.55.

$$B_g(\theta, \theta_m) = B_0 \cos(Z_r(\theta - \theta_m)) - B_1 \cos(p_{mod}^- \theta + Z_r \theta_m) - B_1 \cos(p_{mod}^+ \theta - Z_r \theta_m) \quad (6)$$

Considering the winding span of the fractional slot winding configuration and by using the Faraday's law with (6), the back EMF of SPM vernier machine can be obtained as (7), where ω_m is the mechanical angular speed of the rotor, N_{ph} is the number of turns per phase, D_g is the air-gap diameter, l_{stk} is the stack length of the machine, k_{w1} is the fundamental winding factor, G_r^\pm is the gear ratio $G_r^\pm = Z_r / p_{mod}^\pm$ and k_{leak} is the leakage factor that is a function of the PM thickness and PM pole pitch.

$$E_{ph} = \omega_m N_{ph} D_g l_{stk} F_{m1} k_{w1} k_{leak} [P_0 + 0.5P_1 (G_r^- - G_r^+)] \sin(Z_r \theta_m) \quad (7)$$

2.2. Specific Electric Loading and Torque Density

The specific electric loading, alternatively called surface current density, is commonly represented by the symbol K_s , and it can be expressed as (8), where m is the number of phases and I_{ph} is the RMS value of the phase current. The choice of K_s has significant effect on the key electromagnetic performances of a machine, i.e., power factor, torque density, magnetic saturation. While designing an electric machine, it is a very common practice to decide the value of surface current density empirically [7], but it is not suitable especially for the flux modulation machines. It will be shown in the upcoming sections that depending on the design parameters the optimal value of K_s varies with the slot-pole combination of the machine.

$$K_s = \frac{2}{\pi} \frac{m N_{ph} I_{ph}}{D_g} \quad (8)$$

Under the condition that the applied current is in phase with the back EMF of (7), the machine produces the maximum torque, and thus the torque per rotor-volume (in case of outer rotor, air-gap volume), TRV is obtained as given by (9). From (9), it is clear that for a given winding configuration and magnet material having specific B_r , the TRV of SPMVG is proportional to the available surface current density K_s , the gear ratio of the machine and the choice of slot-pole combination which affects the value of g_{eff} and β .

$$TRV = 1.8 k_{w1} K_s B_r \frac{\mu_0}{g_{eff}} [1 + (0.52G_r^- - 0.52G_r^+ - 0.8)\beta] \quad (9)$$

2.3. Flux Densities of Teeth and Back Yoke

To avoid the saturation problem, the flux density in the iron core parts should be kept constant. In order to estimate the flux density levels in the iron core parts of the machine in operation, it is important to consider both the MMF sources, i.e., the PMs and the stator windings which are configured to utilize the modulation flux having pole p_{mod}^- pairs. Under the condition of maximum torque per ampere, the PM MMF F_m and the stator windings MMF F_w will be orthogonal to each other; thus, the net air-gap MMF F_g can be expressed as (10), where F_{w1} is expressed as (11) having the term of surface current density K_s .

$$F_g = F_m + F_w \approx F_{m1} \cos(Z_r(\theta - \omega_e t)) + F_{w1} \cos(p_{mod}^- \theta + \omega_e t - \frac{\pi}{2}) \quad (10)$$

$$F_{w1} = \frac{3\sqrt{2}}{\pi} \frac{k_{w1} N_{ph} I_{ph}}{p_{mod}^-} = \frac{k_{w1} K_s D_g}{\sqrt{2} p_{mod}^-} \quad (11)$$

By using the net air-gap MMF of (10) with the air-gap permeance of (2), the net air-gap flux density $B_{g.net}$ can be obtained as

$$B_{g.net} \approx B_{conv} \cos(Z_r \theta - \omega_e t - \alpha_1) - B_{ver} \cos(p_{mod}^- \theta + \omega_e t + \alpha_2) \quad (12)$$

where $B_{conv} = \sqrt{(P_0 F_{m1})^2 + (0.5 P_1 F_{w1})^2}$, $B_{ver} = \sqrt{(0.5 P_1 F_{m1})^2 + (P_0 F_{w1})^2}$,
 $\alpha_1 = \tan^{-1} \left(\frac{0.5 P_1 F_{w1}}{P_0 F_{m1}} \right)$, $\alpha_2 = \tan^{-1} \left(\frac{P_0 F_{w1}}{0.5 P_1 F_{m1}} \right)$.

By integrating $B_{g.net}$ of (12) over one winding pole area and a tooth area individually, both the back yoke flux and tooth flux are obtained as (13) and (14), respectively, where $k_1 = \frac{B_{conv} D_g l_{stk}}{Z_r} \sin \left(\frac{\pi Z_r}{Z_s} \right)$, $k_2 = \frac{B_{ver} D_g l_{stk}}{p} \sin \left(\frac{\pi p}{Z_s} \right)$. First, it should be noted that both the main and the modulation fluxes contribute to the flux density in the core parts. Depending on the required flux density levels in the stator/rotor yokes, the heights of stator and rotor yoke can be determined by using (13).

$$\phi_{yoke} = r_g l_{stk} \left\{ \frac{B_{conv}}{Z_r} \cos(\omega_e t + \alpha_1) - \frac{B_{ver}}{p} \cos(\omega_e t + \alpha_2) \right\} \quad (13)$$

$$\phi_{teeth} = \sqrt{k_1^2 + k_2^2 + 2k_1 k_2 \cos(\alpha_1 - \alpha_2)} \sin(\omega_e t + \theta) \quad (14)$$

On the other hand, regarding the tooth flux density, as mentioned before, considering the flux modulation effects, the stator slot opening ratio c_0 of SPMVG is generally fixed with a value of 0.5–0.6 at that time the available tooth area is limited; therefore, the tooth saturation problem is tricky to avoid. Using (14), the tooth flux density B_{teeth} can be derived and approximated as (15) since the difference of α_1 and α_2 is normally less than $\pi/3$.

$$\begin{aligned} \hat{B}_{teeth} &= \frac{Z_s}{\pi D_g l_{stk} (1-c_0)} \sqrt{k_1^2 + k_2^2 + 2k_1 k_2 \cos(\alpha_1 - \alpha_2)} \\ &\approx \frac{Z_s}{\pi(1-c_0)} \left\{ \frac{B_{conv}}{Z_r} \sin \left(\frac{\pi Z_r}{Z_s} \right) + \frac{B_{ver}}{p} \sin \left(\frac{\pi p}{Z_s} \right) \right\} \end{aligned} \quad (15)$$

From (15), it is obvious that for a given slot–pole combination (that is, Z_s and Z_r) with a fixed c_0 , the tooth flux density is determined by B_{conv} and B_{ver} which depend on F_{m1} linked with the PM thickness and F_{w1} related with the current density K_s . Because the PM thickness is determined to obtain the maximum back EMF, the teeth saturation can be avoided by careful selection of the surface current density K_s .

In machine design, the maximum tooth flux density is commonly set as 1.8T, but it should be noted that the flux density B_{teeth} of (15) is composed of two fluxes with different wavelengths. To demonstrate the peculiar nature of vernier machine, the conceptual flux density waveforms of regular PM machine with Z_r pole pairs and vernier PM machine with $5Z_r$ pole pairs is shown in Figure 2. If the saturation of iron core is assumed to begin from 1.5T and if both the machines are designed to obtain 1.8T of the tooth flux density, the saturated core area of vernier PM machine is comparatively much smaller than that of the conventional PM machine as depicted in Figure 2. Therefore, when using (15), the flux density can be higher than 1.8 for design of the vernier PM machine.

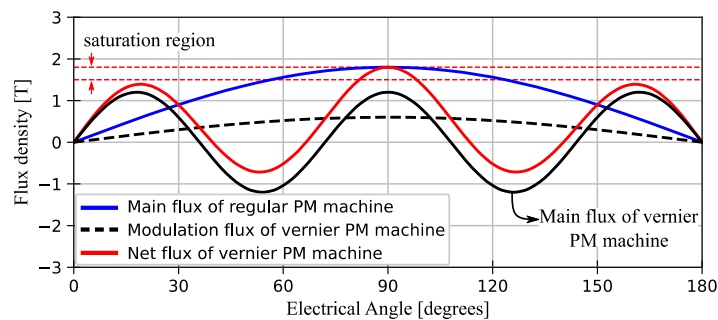


Figure 2. Conceptual distribution of the flux density.

2.4. Inductance and Power Factor

The power factor of a PM machine can be expressed as (16), where X_s represents the synchronous reactance of the machine. As given by (16), the power factor is inversely proportional to the synchronous reactance X_s and the current I_{ph} . It will be shown in the following section that the values of I_{ph} , X_s and E_{ph} vary with the slot–pole combination, and at that time, each slot–pole combination offers a specific power factor as given by (16).

$$PF = \left(\sqrt{1 + \left(I_{ph} \frac{X_s}{E_{ph}} \right)^2} \right)^{-1} \quad (16)$$

The synchronous reactance X_s is related with the average permeance P_0 of (3) and the operating frequency that depends on Z_r . Considering the slot leakage and end turn effects, synchronous reactance X_s is calculated in [7] as given by (17). It can be noted that the X_s is proportional to the PM pole pairs Z_r and hence the gear ratio. From (7) and (17), it is obvious that as the gear ratio increases, both the back EMF and the reactance increase, but the increase in X_s is more than that of the back EMF; therefore, the power factor is inversely related with the gear ratio.

$$X_s = \frac{9\pi}{2\mu_0} \left(\frac{N_{ph}}{Q_s} \right)^2 \frac{D_g I_{stk}}{g_{eff}} Z_r \omega_m \quad (17)$$

3. Nature of the Design Problem and Design Criteria

As discussed in detail, the choice of the specific electric loading K_s has a significant influence on the key electromagnetic performances, and especially the magnetic saturation in the tooth region is also sensitive to the applied specific electric loading. Considering the unique operation principle of PM vernier machine, certain design constraints exist; for example, to keep the modulation flux higher, a slot opening ratio should be kept around 0.5~0.6. As a result of fixed slot opening ratio, the available tooth area is limited and it leads to higher tendency of tooth saturation in PM vernier machine. Furthermore, it is important to keep a specific PM thickness called the optimal PM thickness in order to obtain the maximum back EMF, and obviously higher back EMF is advantageous for both the torque density and the power factor.

In the following section, various performances of SPMVG will be discussed, and it will be shown that the performances are sensitive to certain design parameters. Thus, to effectively utilize the advantages of SPMVG, the proper selection of various design parameters is important. First, in order to demonstrate an important aspect of the design problem, the graph of the gear ratio with variation of the PM pole pairs Z_r and the total stator slots Z_s is shown in Figure 3. Under the condition of balanced 3-phase stator winding configuration, it is possible to operate everywhere on the graph except the infeasible region shown in Figure 3. Now, it is to be decided which slot–pole combination should be selected among the various slot–pole combinations with different gear ratios and modulation pole pairs.

To demonstrate the various trends of the design parameters and electromagnetic performances of SPMVG, three gear ratios ($G_r = 5, 8, 11$) with a range of modulation pole pairs of up to 25 are chosen. As mentioned, the 15 MW DD conventional PM generator designed by NREL [3] is taken as a reference. Initially, in order to comparatively analyze the various aspects of the design parameters and the performances, the basic geometry of the 15 MW reference model (see Table 1) will be used for the SPMVG.

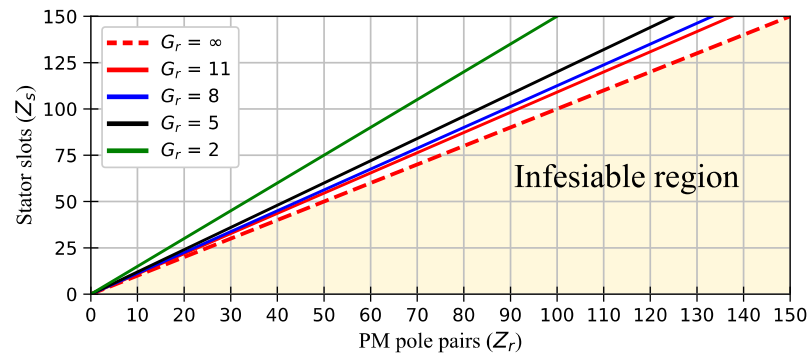


Figure 3. Gear ratio G_r as a function of Z_s and Z_r .

Table 1. Design Parameters.

Parameters		Reference Model [3]	SPM Vernier Machine
Rated Power/Rated Speed	P_{rated}/ω_{rated}	15 MW/7.56 rpm	
Air-gap diameter	D_g	10.16 m	
Air-gap length	g_a	10.16 mm	
Stack length	l_{stk}	2.17 m	1.30 m
PM thickness	g_m	58.39 mm	58.75 mm
Slots/PM pole pairs	Z_s/Z_r	240/100	78/65
Modulation pole pairs	p_{mod}^-	—	13
Surface current density	K_s	92.46 kA/m	85.52 kA/m
Volume current density	J_s	3.39 A/mm ²	
Coil turns per phase	N_{ph}	320	

3.1. Back EMF Performance and Slection of Optimal PM Thickness

The back EMF performance of SPMVG is very sensitive to certain design parameters such as the slot opening ratio c_0 , slot-pole combination, and the PM thickness g_m . To show the back EMF trends, a gear ratio of 11, rated speed of 7.56 rpm, slot opening ratio c_0 of 0.55, air-gap diameter and stack length of the reference model (see Table 1) is used. By using those basic design parameters, the back EMF of SPMVG with variation of PM thickness and modulation pole pairs p_{mod}^- is shown in Figure 4. First, it can be noted that the magnitude of the back EMF is higher when p_{mod}^- is lower, and back EMF starts decreasing as p_{mod}^- increases. Moreover, for each p_{mod}^- there exists a specific PM thickness called the optimal PM thickness that produces the maximum back EMF as shown by the black dotted line in Figure 4, and it should be noted that as the p_{mod}^- increases, the optimal PM thickness starts decreasing.

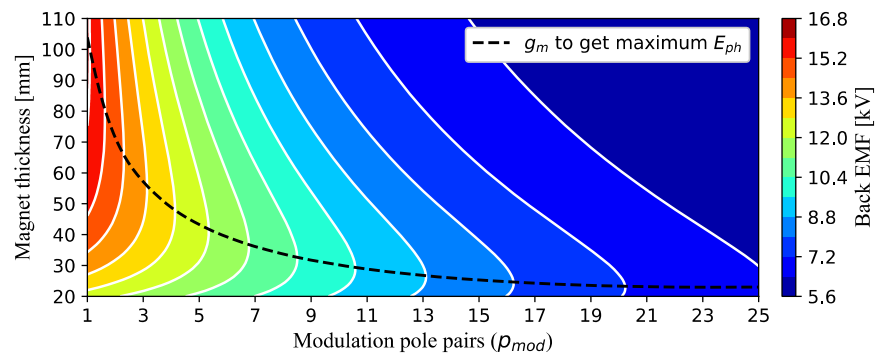


Figure 4. Back EMF contour ($G_r = 11$ and $p_{mod}^- = 1 \sim 25$).

At rated speed of 7.56 rpm, by using (7), the back EMF performance of SPMVG at the optimal PM thickness for the three gear ratios ($G_r = 5, 8, 11$) and their $p_{mod}^- = 1 \sim 25$ is obtained as shown in Figure 5; for comparison, the back EMF of the reference model is also depicted in the graph. First it should be noted that with the same air-gap geometry, the back EMF of SPMVG with each gear ratio and its p_{mod}^- is significantly higher than that of the reference model; obviously, it is due to the additional advantages of the flux modulation effects. Moreover, the back EMF trends suggest that higher gear ratio with lower p_{mod}^- offers the higher back EMF. For a given gear ratio, as the p_{mod}^- increases, the optimal PM thickness thins; as a result, the magnitude of F_{m1} starts decreasing, and the leak factor k_{leak} starts increasing, due to which the back EMF decreases as it is given by (7).

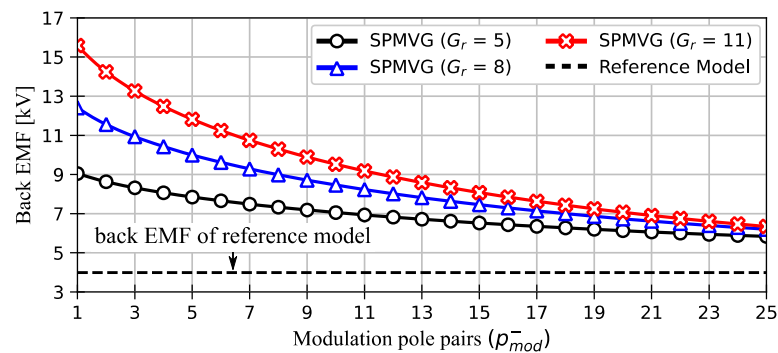


Figure 5. Back EMF calculated at optimal g_m ($G_r = 5, 8, 11$ and $p_{mod}^- = 1 \sim 25$).

3.2. Available Surface Current Density

Unlike the problem of magnetic saturation in the back yoke, the flux density in the tooth region is tricky to control because the available tooth region is limited due to the fixed stator slot opening ratio c_0 . When the optimal magnet thickness obtained in the previous section is used for a given slot–pole combination, the only adjustable variable for B_{teeth} of (15) is the surface flux density K_s . Therefore, it is necessary to determine the proper K_s to keep the value of B_{teeth} in order to avoid the saturation problem. Considering that B_{teeth} of a vernier machine can be higher than that of a conventional one, it is set to $1.8/0.95 = 1.92$ T in this study. Thus, the available surface current density K_s that ensures the constraint of $B_{teeth} = 1.92$ T for each gear ratio and its p_{mod}^- are obtained and shown in Figure 6. It can be noted that the available K_s is somewhat inversely proportional to G_r and is almost proportional to p_{mod}^- . In addition, the results in Figure 6 clearly explain why it is not proper to take commonly used K_s value of the reference model, and notes that K_s for SPMVG can be much smaller depending on its slot–pole combination.

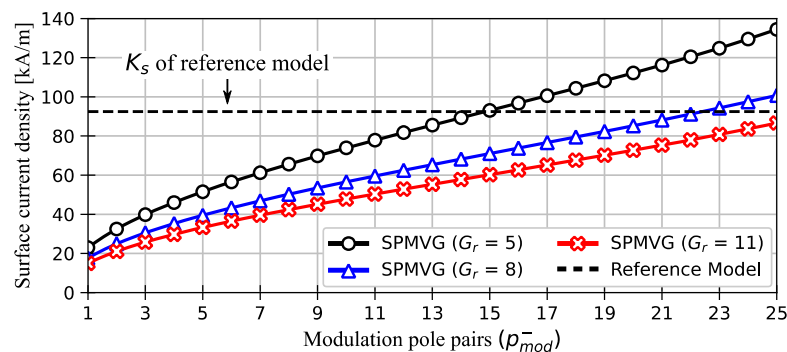


Figure 6. Available surface current density K_s ($G_r = 5, 8, 11$ and $p_{mod}^- = 1 \sim 25$).

3.3. Torque Density and Power Factor

As the SPMVG has to be designed for a rated power of 15 MW, the rated speed, air-gap diameter, air-gap length, number of turns and volume current density of SPMVG are set

the same as those of the reference model (see Table 1). Under those design constraints, by using the calculated available surface current density for SPMVG, the required stack length l_{stk} for rated power of 15 MW is calculated as shown in Figure 7. It can be noted that for the same rated power, as the number of modulation pole pairs p_{mod}^- increases, the required stack length of SPMVG first decreases, and at higher number of p_{mod}^- it starts increasing, regardless of the higher K_s . Moreover, it can be seen that the lower gear ratio offers more advantage in terms of lower l_{stk} due to the fact that the available K_s increases as the gear ratios decreases. The stack length of the reference model is also depicted in Figure 7. It can be noted that for the same rated power, SPMVG, depending on the gear ratio and number of modulation pole pairs, mostly offers much lower stack length that that of the reference model.

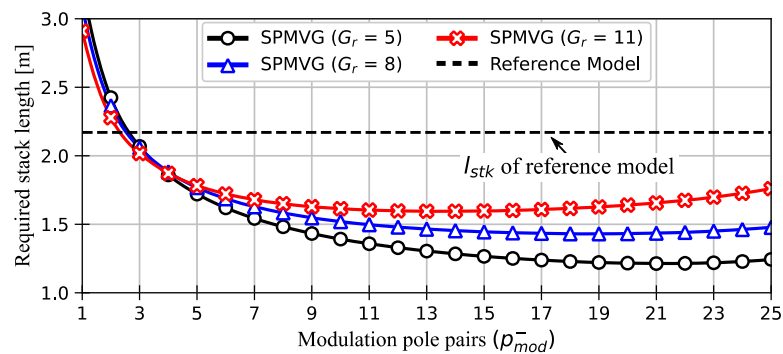


Figure 7. Required stack length l_{stk} for 15 MW ($G_r = 5, 8, 11$ and $p_{mod}^- = 1 \sim 25$).

The torque per air-gap volume commonly known as TRV is calculated by using (9) as shown in Figure 8; the TRV of the reference model is also depicted on the graph. It can be noted that each gear ratio and its modulation pole pairs p_{mod}^- , depending on the available surface current density K_s , offer a certain TRV, and as the modulation pole pairs p_{mod}^- change, the available TRV changes significantly. As compared to the TRV of the reference model, that is, 110.38 kPa, the SPMVG with $G_r = 5$ and $p_{mod}^- = 21$ offers up to 80% higher TRV that is quite significant. As shown in Figure 8, it should be noted that at lower number of p_{mod}^- , higher gear ratios, despite their lower K_s , provide comparatively higher TRVs, but as p_{mod}^- starts increasing, lower gear ratio has a clear advantage of having higher TRV. Furthermore, as shown in Figure 8, it can be noted that at higher number of modulation pole pairs, especially for higher gear ratios, the TRV starts decreasing despite having higher available K_s . In fact, it is due to the fact that at higher number of p_{mod}^- , the PM-PM leakage flux is significant, and so is the decaying back EMF due to lower magnitude of F_{m1} and P_1 .

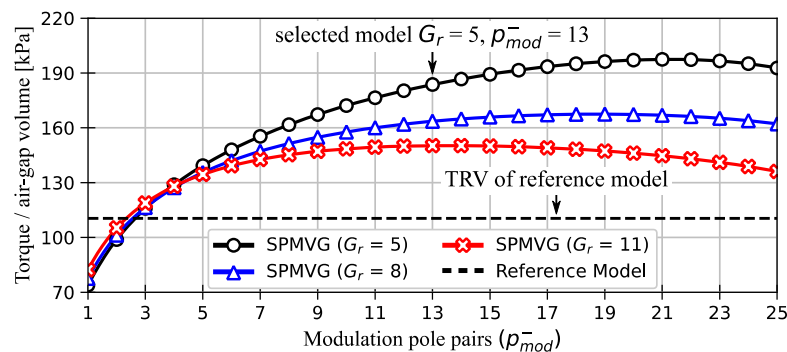


Figure 8. Variation of TRV ($G_r = 5, 8, 11$ and $p_{mod}^- = 1 \sim 25$).

As discussed before, the available surface current density has direct and the back EMF has inverse relation with the modulation pole pairs p_{mod}^- ; thus, from (16) it is obvious that the power factor will decrease as the p_{mod}^- will increase. The calculated power factor of

SPMVG for the three gear ratios and their p_{mod}^- is shown in Figure 9; it can be seen that the power factor starts decreasing as the p_{mod}^- increases, and of course the power factor is inversely related with the gear ratio. Moreover, it can be noted that the power factor of the SPMVG is much lower in comparison with the reference model. It is interesting to note that, considering the power factor, it is better to use lower p_{mod}^- that is a conflicting problem with the TRV.

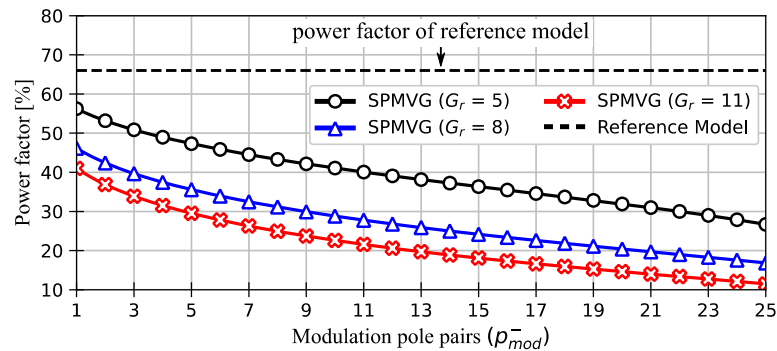


Figure 9. Variation of power factor ($G_r = 5, 8, 11$ and $p_{mod}^- = 1 \sim 25$).

Considering the TRV, it is better to operate at higher number of modulation pole pairs p_{mod}^- ; however, at higher p_{mod}^- , apart from the worse power factor, there exists few more limitations including the PM-PM leakage flux and the PM demagnetization issues. As the PM-PM leakage flux is directly proportional to the number of PM pole pairs, at higher number of p_{mod}^- , due to the increased leakage flux, the machine performance starts decreasing as can be observed in Figure 8; at higher number of p_{mod}^- , despite having higher available K_s , the TRV starts decreasing. Moreover, as mentioned before, as p_{mod}^- increases, the optimal PM thickness decreases, and due to the higher surface current density, the winding MMF increases. Both these factors, i.e., thin PM thickness and higher demagnetization force clearly indicate the concerns of the PM demagnetization at higher number of modulation pole pairs. Therefore, considering the practical limitations of having the low power factor and the PM demagnetization, it is feasible to design the machine with a lower gear ratio and moderate number of p_{mod}^- depending on the required TRV or power factor.

The main focus of the study is to propose a systematic design procedure with the aim to properly choose the various entailed design parameters. In that regard, first, the key analytical expressions were obtained, and it was shown that the main electromagnetic performances such as the TRV, power factor and flux density in the core parts are directly linked with the choice of specific electric loading. Therefore, it is very important to properly choose the specific electric loading to effectively utilize the advantages of SPMVG while avoiding problems such as core saturation, PM demagnetization and excessively lower power factor. To deal with those concerns, a design criterion under some design conditions is developed, which clearly shows that depending on certain design parameters, each slot–pole combination corresponds to a certain value of specific electric loading. Thus, it is obvious that each slot–pole combination and the resulting gear ratio of SPMVG offers a certain TRV and power factor. By using the developed design criteria, with variation of the slot–pole combination, the key electromagnetic characteristics and design parameters such as the back EMF characteristic at optimal PM dimensions, available surface current density, TRV and power factor trends are thoroughly discussed. The obtained results, especially the TRV and the power factor variation trends, provide a clear guide for the selection of the gear ratio as well as the number of modulation pole pairs. It was clearly shown that considering the TRV and the power factor, it is better to use lower gear ratio; however, the selection of the number of modulation pole pairs p_{mod}^- is a compromising problem between the TRV and the power factor.

In this study, with the aim to achieve maximum TRV while having a power factor limit around 40%, the SPMVG with a gear ratio of 5 and $p_{mod}^- = 13$ is selected as depicted in Figure 8. The detailed design parameters of the selected SPMVG model in comparison with the reference model are given in Table 1. From the comparison of the stack length and the surface current density of SPMVG with that of the reference model, it is important to note that the SPMVG with much lower air-gap volume and reduced value of surface current density is providing the same rated power of 15 MW. In fact, it highlights the specific nature of the SPMVG and of course the additional advantages of the flux modulation effects.

4. FEM Modeling and Results

The detailed geometry of the reference model is specified in [3], the main design parameters of both the reference model and the SPMVG are given in Table 2, and by using those parameters, both the generators are modeled in 2D-FEM. Firstly, for both the prototype models, the stator winding configuration and the no-load flux lines with the specified PM thickness are shown in Figure 10, where the letters A, B and C represent the three phases and the signs show the direction of the winding conductors. At the same rated speed of 7.56 rpm, the back EMF waveforms of both the prototype models are calculated and compared as shown in Figure 11. The magnitude of the fundamental components of the back EMF waveforms are given in Table 2. It can be noted that at the same rated speed, despite much smaller dimensions of SPMVG, its back EMF is almost similar to that of the reference model. It is due to the additional advantages of the flux modulation effects.

Table 2. Performance Summary.

Parameters	Reference Model	SPM Vernier Machine
Back EMF (RMS)	3.99 kV	3.92 kV
Average Torque		19.42 MNm
Torque/Volume (TRV)	110.38 kPa	184.26 kPa
Torque Ripple	1.61%	8.57%
Power Factor	66.68%	37.14%
Efficiency	96.55%	96.40%

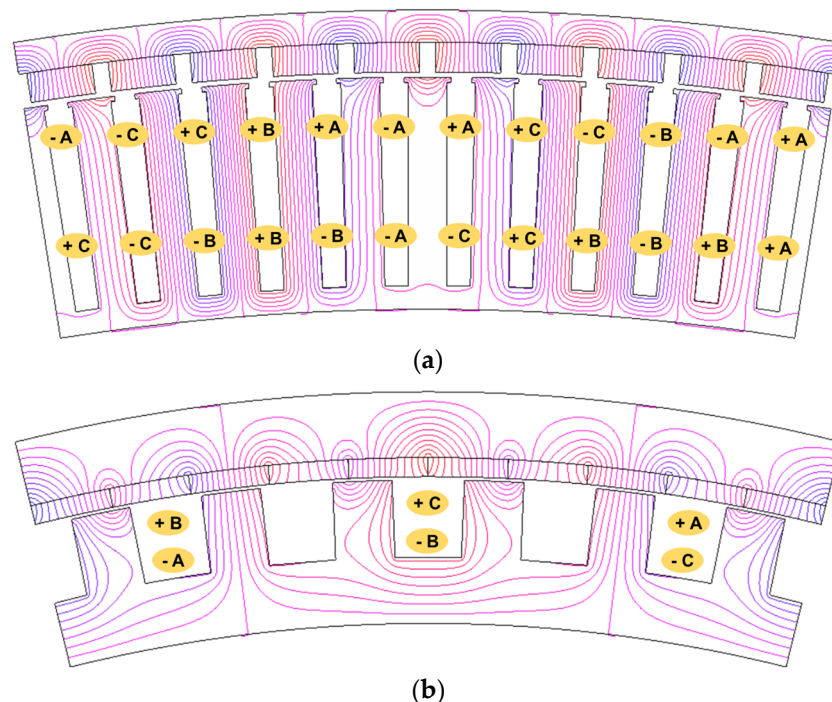


Figure 10. No-load flux lines (a) reference model, (b) designed SPMVG.

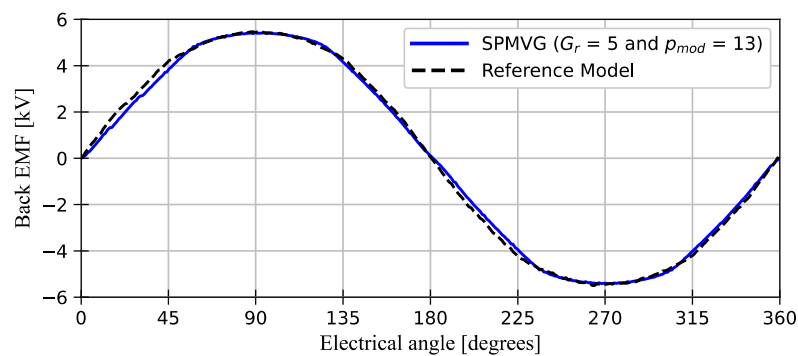


Figure 11. Comparison of back EMF waveforms (at $\omega_{rated} = 7.56$ rpm).

At the rated load conditions, the flux density distribution in the cores of the SPMVG and the reference model are shown in Figure 12. It shows that the SPMVGs do not have severe saturation spots, which means the machine is properly designed. Furthermore, for both the prototypes, considering their surface current densities, the corresponding rated current is applied in phase with the back EMF, the resulting torque waveforms are shown in Figure 13, and the percent torque ripple that represents the ratio of peak–peak torque to average torque is calculated for both the prototype models, and the values are given in Table 2.

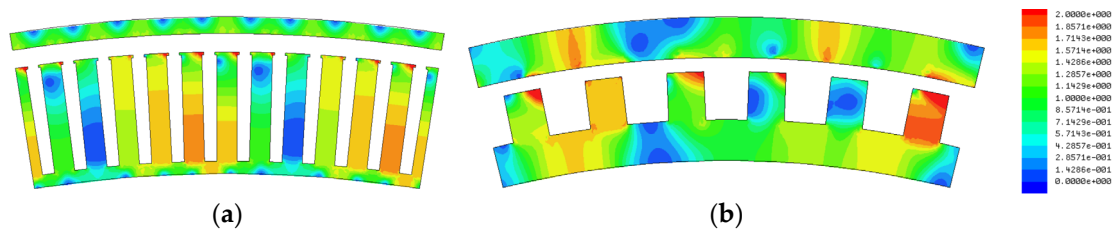


Figure 12. Flux density distribution at rated conditions (a) reference model, (b) designed SPMVG.

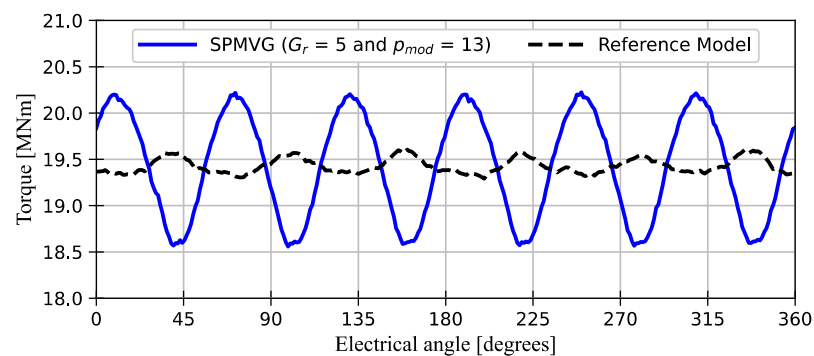


Figure 13. Comparison of torque waveforms.

For both the prototype models, the summary of the electromagnetic performance along with the power factor, TRV and the efficiency is given in Table 2. It can be noted that despite the fact that the K_s of the SPMVG is 7.5% less than that of the reference model, the TRV of the SPMVG is almost 1.67 times higher compared to the reference model. The torque quality of the reference model is comparatively higher than that of the SPMVG but still the torque ripple of the SPMVG is acceptable as the machine is used without any modification in the structure. Moreover, the compromising power factor, as is well known that the power factor of flux modulation machines remains a challenge, the designed SPMVG has a power factor of 0.37. As discussed, it is possible to improve the power factor by compromising the TRV; however, the development of more effective ways of increasing the power factor requires further research. Furthermore, the efficiency of the SPMVG is

calculated by considering the copper and the iron losses, as given in Table 2. The SPMVG offers efficiency that is almost similar to that of the reference model.

Finally, by using the geometrical information of both the generators, the active material consumption for the various generator parts such as PM, copper winding, stator and rotor is obtained as given in Table 3. It can be noted that the designed SPMVG has a clear advantage in terms of the PM material and copper consumption, both of which are comparatively expensive materials. Moreover, the designed SPMVG also has much lower stator steel mass than the reference model; however, the rotor mass of the SPMVG is comparatively higher. From the perspective of the control stability, the higher rotor mass/inertia of the SPMVG is actually advantageous. As given in Table 3, it can be noted that the net generator mass of the SPMVG is 8.5% lower than that of the reference model, which is quite beneficial. It should be noted that the SPMVG structure is used in its most fundamental form, thus there still exists a margin to further lower the material consumption.

Table 3. Active Material Consumption (ton).

Parameters	Reference Model	SPM Vernier Machine
Permanent Magnet	26.54	20.06
Copper Winding	9.01	5.08
Stator Core	153.00	107.32
Rotor Core	38.91	75.62
Total Generator Mass	227.46	208.08

5. Conclusions

In this paper, a surface PM vernier machine (SPMVG) for the application of MW-scale DD wind turbine is designed and analyzed against a conventional SPM DD generator. The various aspects of the design problem are discussed, and it is shown that for each slot–pole combination, the proper choice of certain design parameters such as specific electric loading and PM dimensions are necessary to effectively utilize the advantages of PM vernier machine. By considering the interrelationship between various design parameters, a design criterion under certain design constraints is developed. The developed design criterion ensures the proper selection of various entailed design parameters. By using the developed designed criterion, various electromagnetic performances of SPMVG with variation in the slot–pole combination are presented. It is shown that the surface current density has substantial impact on the various key electromagnetic performances, and it is determined that for each slot–pole combination of SPMVG, there exists a certain value of surface current density. Therefore, each slot–pole combination of SPMVG due to its unique available surface current density offers a certain torque density and power factor which ultimately serves as a guide for the selection of the gear ratio and the number of modulation pole pairs.

Based on the developed design procedure, an SPMVG for a rated power of 15 MW is designed, and its electromagnetic performance is comprehensively analyzed against a counterpart conventional DD generator. It was clearly shown that compared to the reference model, the designed SPMVG has almost 67% less air-gap volume despite its lower surface current density. Moreover, the designed SPMVG has comparatively less active material consumption; however, the only compromise is the 44% lower power factor of SPMVG.

Author Contributions: Conceptualization, B.K. and A.R.; methodology, B.K. and A.R.; software, A.R.; validation, A.R.; formal analysis, A.R.; investigation, A.R.; resources, A.R.; data curation, A.R.; writing—original draft preparation, A.R.; writing—review and editing, B.K. and A.R.; visualization, A.R.; supervision, B.K.; project administration, B.K.; funding acquisition, B.K. All authors have read and agreed to the published version of the manuscript.

Funding: This research was supported in part by Basic Science Research Program through the National Research Foundation of Korea (NRF) funded by the Ministry of Education (Grant NRF-2016R1A6A1A03013567) and in part by Korea Electric Power Corporation (Grant number: R21XO01-6)."

Data Availability Statement: Not applicable.

Conflicts of Interest: The authors declare no conflict of interest.

References

1. Global Wind Energy Council (GWEC). *GWEC Global Wind Report 2022*; GWEC: Brussels, Belgium, 2022.
2. Bortolotti, P.; Tarres, H.; Dykes, K.; Merz, K.; Sethuraman, L.; Verelst, D.; Zahle, F. *IEA Wind Task 37 on Systems Engineering in Wind Energy WP2.1 Reference Wind Turbines*; National Renewable Energy Laboratory: Golden, CO, USA, 2019.
3. Gaertner, E.; Rinker, J.; Sethuraman, L.; Zahle, F.; Anderson, B.; Barter, G.E.; Abbas, N.J.; Meng, F.; Bortolotti, P.; Skrzypinski, W.; et al. *IEA Wind TCP Task 37: Definition of the IEA 15-Megawatt Offshore Reference Wind Turbine*; National Renewable Energy Laboratory (NREL): Golden, CO, USA, 2020.
4. Polinder, H.; Ferreira, J.A.; Jensen, B.B.; Abrahamsen, A.B.; Atallah, K.; McMahan, R.A. Trends in Wind Turbine Generator Systems. *IEEE J. Emerg. Sel. Top. Power Electron.* **2013**, *1*, 174–185. [[CrossRef](#)]
5. Kim, B.; Lipo, T.A. Operation and design principles of a PM vernier motor. *IEEE Trans. Ind. Appl.* **2014**, *50*, 3656–3663. [[CrossRef](#)]
6. Li, D.; Qu, R.; Li, J.; Xiao, L.; Wu, L.; Xu, W. Analysis of torque capability and quality in vernier permanent-magnet machines. *IEEE Trans. Ind. Appl.* **2016**, *52*, 125–135. [[CrossRef](#)]
7. Kim, B. Design method of a direct-drive permanent magnet vernier generator for a wind turbine system. *IEEE Trans. Ind. Appl.* **2019**, *55*, 4665–4675. [[CrossRef](#)]
8. Rehman, A.; Kim, B. Characteristics analysis of consequent pole ferrite magnet vernier machine using novel equivalent magnetic circuit. *IEEE J. Emerg. Sel. Top. Power Electron.* **2021**, *10*, 1823–1833. [[CrossRef](#)]
9. Tlali, P.M.; Wang, R.-J.; Gerber, S.; Botha, C.D.; Kamper, M.J. Design and performance comparison of vernier and conventional PM synchronous wind generators. *IEEE Trans. Ind. Appl.* **2020**, *56*, 2570–2579. [[CrossRef](#)]
10. Kim, B.; Lipo, T.A. Analysis of a PM Vernier Motor with Spoke Structure. *IEEE Trans. Ind. Appl.* **2016**, *52*, 217–225. [[CrossRef](#)]
11. Padinharu, D.K.K.; Li, G.J.; Zhu, Z.Q.; Foster, M.P.; Stone, D.A.; Griffo, A.; Clark, R.; Thomas, A.S. Scaling effect on electromagnetic performance of surface-mounted permanent-magnet vernier machine. *IEEE Trans. Magn.* **2020**, *56*, 8100715. [[CrossRef](#)]
12. Atallah, K.; Rens, J.; Mezani, S.; Howe, D. A novel “pseudo” direct-drive brushless permanent magnet machine. *IEEE Trans. Magn.* **2008**, *44*, 4349–4352. [[CrossRef](#)]
13. Padinharu, D.K.K.; Li, G.J.; Zhu, Z.Q.; Clark, R.; Thomas, A.S.; Azar, Z. System-level investigation of multi-MW direct-drive wind power PM vernier generators. *IEEE Access* **2020**, *8*, 191433–191446. [[CrossRef](#)]
14. Padinharu, D.K.K.; Li, G.J.; Zhu, Z.Q.; Clark, R.; Thomas, A.; Azar, Z.; Duke, A. Permanent magnet vernier machines for direct-drive offshore wind power: Benefits and challenges. *IEEE Access* **2022**, *10*, 20652–20668. [[CrossRef](#)]
15. Tlali, P.; Wang, R.-J. Prospect of PM Vernier Machine for Wind Power Application. *Energies* **2022**, *15*, 4912. [[CrossRef](#)]

Disclaimer/Publisher’s Note: The statements, opinions and data contained in all publications are solely those of the individual author(s) and contributor(s) and not of MDPI and/or the editor(s). MDPI and/or the editor(s) disclaim responsibility for any injury to people or property resulting from any ideas, methods, instructions or products referred to in the content.